Volume 1 | Number 1 | Jan 2013 | Pages 1–100

PCCP

Physical Chemistry Chemical Physics
www.rsc.org/pccp

ROYAL SOCIETY OF CHEMISTRY

ROYAL SOCIETY OF CHEMISTRY

www.rsc.org/pccp

Journal Name

ARTICLE TYPE

Towards the first theoretical scale of the *trans* effect in octahedral complexes[†]

Frédéric Guégan[*a,b], Vincent Tognetti[c], Laurent Joubert[c], Henry Chermette[a], Dominique Luneau[b] and Christophe Morell[*a]

In this paper, we show that the *trans* effects in octahedral complexes can primarily be related to differences in the ability, for a given ligand, to cede electron density to the metal cation under the influence of the ligand on the *trans* position. Using tools from conceptual DFT or from related paradigms, we highlight this effect on a set of representative examples and further provide the basis for a computational *trans* effect scale. This quantification notably retrieves the experimental *trans* orienting series.

1 Introduction

The Kinetic *Trans* Effect (KTE), sometimes simply called "*trans* effect", is a well-known phenomenon in coordination chemistry since its discovery in 1926[1]. It is characterised by the increase in the substitution kinetics of a ligand in a complex, under the influence of the ligand on the opposite coordination position (whence the label "*trans*")[2,3]. A static analogue to this effect is also known: the Structural *Trans* Effect (STE), sometimes called "*trans* influence"[4]. It is characterised by an increase of a metal-ligand bond length, under the influence of the ligand on the opposite coordination position.

Both STE and KTE are frequently epitomised by square planar complexes, with a d^8 electronic configuration of the metal cation[5], and octahedral complexes, with either a d^6 or d^0 metal electronic configuration[6]. More rarely, they can be observed for lanthanide[7], actinide[8,9] or even iodine[10,11] complexes. These two effects are known to be a likely cause of several chemical properties, ranging from catalytic activity and selectivity[12–14] to metalloprotein reactivity[15–18] and anti-tumoral activity[19–21].

As such, understanding the origin and mechanisms beneath both the STE and KTE seems necessary. Many experimental and theoretical works have been dedicated to this task and, to our best knowledge, have not been fully conclusive yet. All these efforts can be traced back to the 1930's when an electrostatic model[22–25] was proposed, based on polarisation effects between the central metal and ligands. However, its conclusions are generally in contradiction with the outcome of a later model by Chatt, Dewar and Duncanson (CDD)[26,27]. The CDD model, even though elegant, only works for KTE observed with π-acceptor ligands and is unable to account for the generality of the *trans* effects.

Eventually, some other authors tried to correlate metal-ligand σ or π bond strength to the *trans* effects using experimental evidences, such as direct measurements of UV charge transfer bands[28,29]. Lately, many different theoretical works have confirmed that both electron donations and back-donations[30,31] are acting beneath the KTE of square planar complexes, the former by destabilising the complex, the latter by stabilising the transition states of metathesis[32]. Yet, such confirmations are still needed in the case of octahedral complexes.

There is no apparent reason why the same line of argument might not to be applied. Furthermore, it is plain to see that there is a common ground for all these approaches. In all cases indeed, *trans* effects can be understood in terms of electron density deformations. For instance, within the CDD model, *trans* effects are investigated by monitoring the electron transfers from the metal to the ligands. Similarly, in the electrostatic approach, the dipole moment arises from an electron density distortion due to charge accumulation or depletion on given sites. In the case of the donation/back-donation scheme, the extent of electron density shared between the ligand and the metal, as compared to the case of isolated species, could be the relevant parameter to follow.

Conceptual DFT[33–35] (C-DFT) is an elegant framework for characterizing such effects. It expresses the chemical properties of a given system through a set of quantum descriptors. These are based on the response of either the energy or the electron density to external perturbations[36]. Obviously, such a framework

[a] Université de Lyon, Institut des Sciences Analytiques, UMR 5280, CNRS, Université Claude Bernard Lyon 1, 5 rue de la Doua, 69100 Villeurbanne, France
[b] Université de Lyon, Laboratoire des Multimatériaux et Interfaces, UMR 5615, CNRS, Université Claude Bernard Lyon 1, 22 avenue Gaston Berger, 69622 Villeurbanne, France
[c] Normandy University, COBRA UMR 6014 & FR 3038, Université de Rouen, INSA Rouen, CNRS, 1 rue Tesniére 76821 Mont St Aignan, Cedex, France

is adapted to an in-depth investigation of the physical roots of the *trans* effects for octahedral complexes. Two tools are particularly well fitted to monitor the variations of the electron density, namely the Dual Descriptor (DD)[37–39] and the Extended Transition State - Natural Orbitals for Chemical Valence[40–42] (ETS-NOCV). The latter does not strictly belong to C-DFT, still it uses a density deformation matrix and therefore its theoretical framework is quite close to C-DFT. These two indexes combined together have proved very efficient to characterise, understand and rationalise the electron density evolution during a chemical process[43,44].

In this work, the results of a combined DD/ETS-NOCV survey are reported. In a first part, the physical bases for both descriptors are briefly recalled (see the ESI for more details). In a second part the methodology to unravel the STE and KTE is presented. It is then applied on a set of representative examples. The third part is dedicated to the elaboration of a semi-quantitative scale of *trans* orienting groups. The paper ends with some concluding remarks.

2 Theoretical backgrounds

2.1 State Specific Grand Canonical Dual Descriptor

The usual Dual Descriptor $\Delta f_{usual}(\mathbf{r})$[45] is defined as the second derivative of the electron density $\rho(\mathbf{r})$ with respect to the number of electrons N, at frozen geometry (the external potential $v(\mathbf{r})$ remaining constant).

$$\Delta f_{usual}(\mathbf{r}) = \left(\frac{\partial^2 \rho(\mathbf{r})}{\partial N^2} \right)_{v(\mathbf{r})} \tag{1}$$

It allows to characterise, in a single representation, regions within a molecule that are prone to cede ($\Delta f(\mathbf{r}) < 0$) or receive ($\Delta f(\mathbf{r}) > 0$) electron density, the so-called nucleophilic and electrophilic regions in organic chemistry[38,46], and its use to understand the reactivity of organometallic complexes[47,48] has recently been advocated.

Several approximations of the DD are found in the literature, and are developed in the ESI. Here, we use a recently devised formulation, the so-called the "state-specific" approach[49–51], where the DD is identified to a sum of electron density differences between the nth excited and the ground states - the so called nth state specific DDs. Indeed, most of the limitations of the usual approximations are avoided in this formalism; noticeably, the eventual orbital degeneracy is no longer a problem, nor the spin states of the molecules and their associated $N+1/N-1$ forms (see the ESI for more details). Furthermore, the DD within this approach is expected to take into account polarisation effects[52], and as such to represent more accurately reactivity. More specifically, we focus on the first state specific DD $\Delta f_1(\mathbf{r})$, which usually conveys the major contribution to reactivity:

$$\Delta f_1(\mathbf{r}) = \rho_1(\mathbf{r}) - \rho_0(\mathbf{r}) \approx \Delta f(\mathbf{r}) \tag{2}$$

Here, we are interested in comparing chemical systems with different numbers of electrons N. Equations (1) and (2) hold only for a fixed N value (canonical ensemble), and a Legendre transform to the grand-canonical ensemble is needed if one wants to set N as a free parameter. The result of such a transform has

already been reported[50] (and the details are recapped in the ESI), and it can be shown that one simply needs to divide the canonical DD by the square of the molecular hardness η in order to get the Grand-Canonical Dual Descriptor (SS-GCDD) $\Delta s(\mathbf{r})$:

$$\Delta s(\mathbf{r}) \approx \frac{\Delta f(\mathbf{r})}{\eta^2} \approx \frac{\rho_1(\mathbf{r}) - \rho_0(\mathbf{r})}{\eta^2}. \tag{3}$$

For the sake of simplicity and concision, in the following we will refer to the SS-GCDD as the DD.

2.2 DD partition into reactive domains

In order to extract the meaningful chemical information contained within the DD, it is relevant to partition it into domains of constant sign $D_i^{\pm}$, associated to a univocal and specific reactivity. More precisely, all points belonging to a given D_i^+ (respectively D_i^-) feature a positive (resp. negative) DD value and are surrounded by neighbours exhibiting the same DD sign, that corresponds to a predominant electrophilic (resp. nucleophilic) behaviour.

Such a real space partition can be achieved using Domains, a recently developed code[53]. In the latest version of the program, two thresholds are implemented in order to get a clearer picture of the domains. The first threshold, τ_r, excludes from the domains any point in space that would be closer than τ_r to any nucleus. This allows to withdraw the contribution of core regions, which are not expected to contribute significantly to the reactivity, or which may not be accurately described (with the use of pseudo-potentials). The second threshold, τ_{DD}, allows a better separation of the domains by excluding any point in space associated to a norm of the DD that is inferior to τ_{DD} (lower boundary). This permits an efficient delimitation of the reactive sites.

It is possible to integrate the DD within these domains, and thus to gain a deeper insight on the reactivity of the corresponding sites. More precisely, it is possible for each domain $D_i^{\pm}$ to compute its volume, $V_{D_i^{\pm}}$, the integrated value of the DD within this volume, $\Delta s(D_i^{\pm})$, and the average value of the DD in the domain, $\overline{\Delta s(D_i^{\pm})}$. This last value is expected to yield the most valuable information on the domain reactivity, since it shares the same unit as the DD. As we will show in the last part, those average values will actually be the basis for a quantification of the *trans* effect.

2.3 Extended Transition State - Natural Orbitals for Chemical Valence (ETS-NOCV)

The NOCV Ψ_i are the eigenvectors that diagonalise the deformation density $\Delta \rho(\mathbf{r})$ two isolated fragments undergo when they are put into interaction. Mathematically speaking this can be translated by:

$$\Delta \rho(\mathbf{r}) = \sum_m v_m \left[-\Psi_{-m}(\mathbf{r})^2 + \Psi_m(\mathbf{r})^2 \right]. \tag{4}$$

Practically, the NOCVs permit a decomposition of the electron density deformation on the basis of the orbitals of each isolated fragment. It therefore helps to monitor the evolution of the electron density during a chemical process. For instance, it is possible to distinguish between σ and π bonding, and also to separate donation and back-donation effects[54]; physics beneath the

interactions is thus unveiled. In addition to this decomposition of the electron density transfers, an assessment of the associated energetic stabilisation is possible, through the framework of the Extended Transition State[55].

2.4 Computational details

All the complexes structures presented in this work have been fully optimized without symmetry restrictions at the B3LYP level of theory using Gaussian09 package[56]. Pople basis sets are used for all the coordinating atoms: 6-311+G(d) for S and P atoms, 6-311G(d) for the other ones. Metal cations are modelled with the Stuttgart-Dresden Electron Core Potentials (ECP) and corresponding basis set (keywords SDD in Gaussian09)[57]. Frequency calculations have been performed at the same level of theory to ensure the obtained geometries correspond to genuine minima of the potential energy hyper-surface (the coordinates are reported in the ESI). To evaluate the DDs, the first ten excited states have been computed using the Time Dependant DFT framework (TD-B3LYP), and the DD has been subsequently evaluated using equations (2) and (3)[49]. Chemical hardness has been approximated as $\eta = E_{LUMO} - E_{HOMO}$. Condensations were made using Domains[53], and the the same thresholds values were used for all complexes: $\tau_{DD} = 0.2$ a.u and $\tau_r = 0.5$ a.u.

To ensure that computed DD are reliable, they have been also calculated using two other exchange-correlation functionals (PBE0 and M06-2X) for a few complexes. As expected the results are very similar and make the DD a trustable descriptor. In the same spirit, the adequacy of the basis sets and ECP has been confirmed by additional calculations on the cobalt complexes, at the B3LYP/6-311++G(2d,2p) (C, H, N, O) / Wachters+f (Co) level[58,59]. Apart from the computation time, which increases a lot, the tendency remains the same (though the figures change, naturally), hence giving confidence in the adequacy of the computational model. The NOCV calculations have been performed using the Amsterdam Density Functional program (ADF2013)[60], at the B3LYP/TZP-small core level of theory. Both the DD and NOCV density deformations have been represented using GaussView 5[61].

3 *Trans* effect in octahedral complexes

Note: in the following, the labels *trans* and *cis* will refer to the corresponding position in a complex with respect to the strongest *trans* orienting ligand.

3.1 Methodology

The aim of this study is to characterise and rationalize the *trans* effects in octahedral complexes. As pictured in Scheme 1, two approaches have been unfolded. First, the differences in electronic demand between the *cis* and the *trans* positions in a given complex are compared, highlighting the *trans* effect induced by a specific ligand T (left side of the figure). To do so, the geometries of the full complexes are optimised, and afterwards either the *cis* or *trans* ligands L are removed. The DDs of the corresponding incomplete [ML$_4$T] complexes are computed, as well as the NOCVs associated to the coordination of the removed ligands. As exem-

plified in the following, this approach permits to characterise the STE, where one often compares two bond lengths in the same complex (inner reference).

Second, we compare the electronic demand on the *trans* positions in two similar [ML$_5$T] and [ML$_5$T'] complexes, differing only by the *trans* orienting ligands T and T'. A similar approach as previously was used: a first optimisation of the structure, followed by the removal of the *trans* ligands. The DDs of the corresponding fragment complexes [ML$_4$T] and [ML$_4$T'] are calculated, as well as the NOCVs associated to the coordination of the removed *trans* ligands. This approach likely allows to characterise the KTE, where one usually compares two complexes only differing by the *trans* orienting ligand.
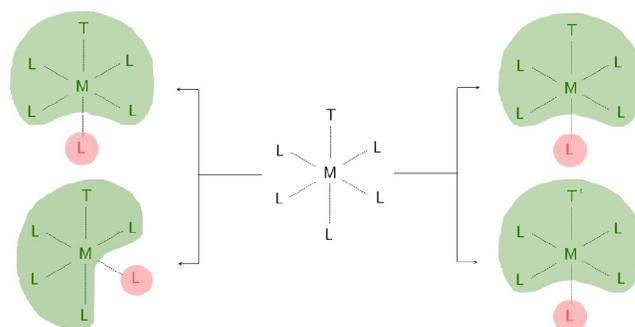
Scheme 1 Schematic representation of the applied methodology; left side, highlight of the differentiation between *trans* and *cis* ligands. Right side, comparison between two *trans* orienting groups T and T'.

The validity of these approaches is supported by the fact that ligand substitutions in octahedral complexes generally proceed via dissociative mechanisms. [ML$_5$] moieties therefore bear some chemical meaning as potential intermediates[2]. In the following discussion, the two approaches are developed in order to assess the efficiency of both tools (DD and NOCV) to retrieve and rationalise the *trans* effects. The complexes listed in table 1 have been chosen to be representative of the variety both *trans* effects offer, either in electronic configuration (d^0 and d^6 for the STE, d^6 for the KTE), period of the metal (4 and 5) or ligand nature (σ or π donor, π acceptor).

Table 1 List of the studied complexes. Complex S3 is given in ESI. * L= dimethylaminocarbene.

Label	Formula	Specificity
1	$[Co(NH_3)_2(NO_2)_3(CH_3)]^-$	STE, d^6, σ donors
2	$[NbO(SCN)_5]^{2-}$	STE, d^0, σ, π donors
3-H$_2$O	$[Rh(NH_3)_4(H_2O)_2]^{3+}$	KTE, d^6, σ donors
3-Cl	$[Rh(NH_3)_4(H_2O)Cl]^{2+}$	KTE, d^6, σ, π donors
4-OH	$[Co(en)_2(H_2O)OH]^{2+}$	KTE, d^6, σ, π donors
4-SO$_3$	$[Co(en)_2(H_2O)SO_3]^+$	KTE, d^6, π acceptor
S3*	$[RhL(PMe_3)_2Cl_3]$	STE, d^6, σ, π donors

3.2 Comparing *cis* and *trans* positions

3.2.1 A first example of a d^6 STE complex: $[Co(NH_3)_2(NO_2)_3(CH_3)]^-$

The first chosen example, $[Co(NH_3)_2(NO_2)_3(CH_3)]^-$ (**1**) is known to show a marked STE[62] due to the methyl ligand. Indeed, the Co(III)-NO_2^- bond length is 0.10 Å longer *trans* to CH_3^- than *cis*. Two $[ML_5]$ fragments have been built by removing either the *trans* or a *cis* nitrito ligand. The DDs computed for the fragments are presented in figure 1. The similarity between the metal contributions to the DD in both fragments is striking. They comprise a nucleophilic part reminiscent of a non-bonding metal d orbital, and an electrophilic part developing towards the coordination vacancy. The latter feature could be expected: removing a ligand, *i.e.* a nucleophile, will logically exacerbate the electrophilicity of the remaining $[ML_5]$ species.
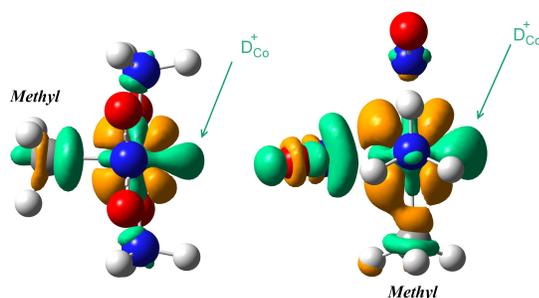
Fig. 1 DD isosurfaces for the $[ML_5]$ fragments deriving from complex **1**. Left: **1-trans**, deprived from the *trans* nitrito group with respect to methyl, $-0.4 \leq \Delta s(\mathbf{r}) \leq 0.4$ a.u. Right: **1-cis**, deprived from the *cis* nitrito with respect to methyl, $-0.2 \leq \Delta s(\mathbf{r}) \leq 0.2$ a.u. Surfaces colours: orange, $\Delta s(\mathbf{r}) < 0$; green, $\Delta s(\mathbf{r}) > 0$. Colour scheme: red, O atoms; blue, N atoms; grey, C atoms; white, H atoms: lavender, Co atoms. Coordination vacancies are directed on the right side of each $[ML_5]$ fragment, and green arrows point towards the D_{Co}^+ domains. Methyl ligands are highlighted.

Table 2 DD condensation for $[ML_5]$ fragments deriving from complex 1. All values in atomic units.

	1-cis	1-trans
$\Delta s(D_{Co}^+)$	145.6	21.4
$V(D_{Co}^+)$	24.1	17.6
$\overline{\Delta s(D_{Co}^+)}$	6.04	1.22

This electrophilic basin looks noticeably larger in **1-cis** than in **1-trans**, even using an isovalue that is twice higher. The results of the condensation on these domains is summarised in table 2. In the case of **1-trans**, the integrated value is about 7 times smaller than that of **1-cis**. The volume of the domain is also smaller for **1-trans**, but in a much weaker proportion (roughly 30%). In the end, the mean value of the DD $\overline{\Delta s(D_{Co}^+)}$ is much higher for **1-cis** than **1-trans**. The *trans* position, being much less electrophilic than the *cis* one, is then expected to stabilise less efficiently ligands: the associated metal-ligand bond is expected to be longer.

This is in total compliance with experimental results. This could also be retrieved using NOCVs for the coordination of ni-

trite to the $[ML_5]$ fragments. The deformation density associated to the first (and main) NOCV pair is represented on figure 2. In both cases the incoming ligand (NO_2^-) loses electron density, which relocates between the ligand and the cobalt atom: a cobalt-nitrite bond is formed. Furthermore, some internal relocations are observed on the $[ML_5]$ moiety.

Those can be seen as the withdrawal of an excess of electron density that was transferred from the ligands to the metal cation to counteract the coordination vacancy. Coordination of the *cis* nitrito is associated to a NOCV (± 1) energetic stabilisation of 40.1 kcal/mol and a transfer of 0.66 electrons. On the other hand, coordination of the *trans* nitrito is associated to an energetic stabilisation of 31.3 kcal/mol and a transfer of 0.57 electrons. The metal-ligand bond is then weaker on the the *trans* position, and as such we retrieve the expected STE.
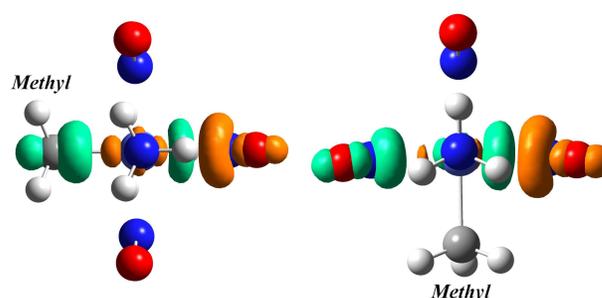
Fig. 2 Deformation density for the first NOCV pair, associated to the coordination of a nitrito ligand to **1-trans** (left) and **1-cis** (right). Isovalue: $\Delta\rho(\mathbf{r}) = \pm 4.10^{-3}$ a.u. Colour scheme: orange, $\rho(\mathbf{r})$ depletion; green, $\rho(\mathbf{r})$ accumulation. Atom colours and orientations of the fragments were chosen as in figure 1. The incoming ligand is located on the right side of each complex, and methyl ligands are highlighted.

3.2.2 An example of a d^0 STE complex: $[NbO(SCN)_5]^{2-}$

The second example, $[NbO(SCN)_5]^{2-}$ (**2**), is known to exhibit a marked STE due to the oxide ligand[63]: the Nb(V)-SCN^- bond length is 0.18 Å longer *trans* to the oxido as compared to the *cis* position. One can notice the formally d^0 electronic configuration of the metal cation. Similarly to complex **1**, two $[ML_5]$ fragments have been built by removing the *trans* thiocyanate (**2-trans**) or the *cis* one (**2-cis**), and the DD have been computed. The results are displayed on figure 3.

The DD contributions on the metal cation are again similar. Noticeably, the electrophilic part recalls a non-bonding metal d orbital, in perfect line with the previous example. Indeed, in the framework of MO theory, these non-bonding orbitals are empty in the d^0 case, thus likely associated to electrophilicity, and fully occupied in the d^6 case, and associated to nucleophilicity. In the case of **2-cis**, these electrophilic domains are adapted to fit a π-donor ligand, and thus may efficiently stabilise a N-bonding thiocyanate.

2-trans will not offer such a stabilisation: the electrophilic domains develop perpendicularly to the eventual thiocyanate-niobium bond. The *trans* thiocyanate is then expected to be much less stabilised than the *cis* one. Furthermore, the DD lobes on the *trans* thiocyanate in **2-cis** are much more developed than on any
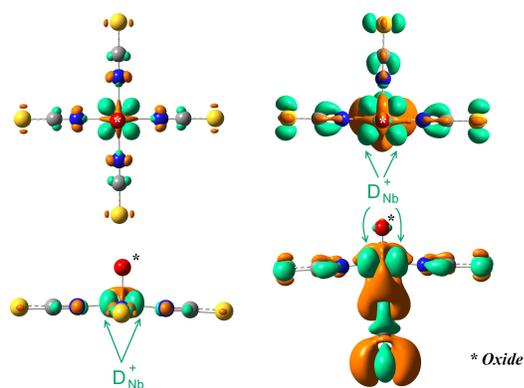
Fig. 3 DD isosurfaces for the [ML$_5$] fragments deriving from complex 2, **2-trans** (left) and **2-cis** (right). Isovalues: $-0.2 \leq \Delta s(\mathbf{r}) \leq 0.2$ a.u. Same colour scheme as in figure 1, the S atoms being depicted in yellow. Top, view along the O-Nb(V) bond ; bottom, side view. Green arrows highlight the D_{Nb}^+ domains, and an asterisk highlights the oxide position.

Fig. 4 Deformation density associated to the first (upper side) and second (lower side) NOCV pairs, for the coordination of a thiocyanate to **2-cis** (left) and **2-trans** (right). Same colour scheme as in figure 2, the incoming ligand being located on the right side. Isovalue: $\Delta \rho(\mathbf{r}) = \pm 4.10^{-3}$ a.u. Oxide ligand positions are highlighted by asterisks.

other one. The aspect is indeed very typical of an isolated SCN⁻ ligand, thus suggesting that this ligand in the complex behaves more like a free ligand than a coordinated one, not to say like a leaving group. Unfortunately, the same partition as previously could not be applied: only negligible values of the DD on the *trans* position could be obtained, since no development of the DD is observed on that position. Actually, this is not a pitfall: if no quantification is possible in that case, one is still able to characterise a *trans* effect.

More insight is gained from the ETS-NOCV study of the coordination of thiocyanate to the [Nb(SCN)$_4$O]⁻ fragments. The results are recapped on figure 4. In the case of the *cis* SCN⁻, the main energetic stabilisation is associated to the formation of a σ bond (NOCV ± 2, -30.4 kcal/mol, 0.47 electrons transferred), but the highest number of transferred electrons is associated to the formation of a π bond (NOCV ± 1, -12.7 kcal/mol, 0.49 electrons). A different tendency is observed for the *trans* SCN⁻: an energetic stabilisation of -18.0 kcal/mol for the σ bond formation (NOCV $\pm$ 1), and 0.34 electrons transferred, -8.1 kcal/mol and 0.52 electrons for the π bond formation (NOCV $\pm$ 2).

Roughly the same numbers of electrons are transferred during the formation of the π bonds, but the associated energetic stabilisation is much higher for the *cis* SCN⁻. Regarding the σ bond formation, both the number of transferred electrons and the energetic stabilisation are higher in the case of the *cis* SCN⁻. Thus one expects the *trans* thiocyanate to be much less stabilised in the complex than the *cis* ones, and as such to be more weakly coordinated: a STE is retrieved.

3.3 Comparing *trans* orienting ligands
3.3.1 An example of a KTE complex: [Rh(NH$_3$)$_4$(H$_2$O)X]$^{n+}$

The two previous examples, in addition to the 3 other examples provided in ESI, confirmed that it is possible to highlight differences between the *trans* and *cis* positions in given complexes, and to relate these differences to a possible STE or KTE. A further step can be taken if one compares two different *trans* orienting ligands, the remains of the complex being conserved.

Let us consider [Rh(NH$_3$)$_4$(H$_2$O)X]$^{n+}$, with X = H$_2$O, n=3 (**3-H$_2$O**) and X = Cl⁻, n=2 (**3-Cl**). It was shown experimentally that water substitution proceeds 5000 times faster for **3-Cl** than for **3-H$_2$O**[64]. In agreement with our methodology, we built two [ML$_5$] fragments based on these two complexes by removing the coordinated water molecule (**ML5-3-H$_2$O** and **ML5-3-Cl**), and computed the corresponding DD, as represented on figure 5. The DD features are very similar to those observed for complex **1**. Noticeably, we retrieve the d AO-type nucleophilic contribution on the metal, and the electrophilic development towards the vacancy. It is not plain whether **ML5-3-H$_2$O** or **ML5-3-Cl** bears the largest contribution at first sight.

Table 3 DD condensation for [ML$_5$] fragments deriving from complex 3. All values in atomic units.

	ML5-3-H$_2$O	ML5-3-Cl
$\Delta s(D_{Rh}^+)$	43.9	21.9
$V(D_{Rh}^+)$	25.2	19.2
$\overline{\Delta s(D_{Rh}^+)}$	1.74	1.14

Results of the condensation are gathered in table 3, and help to answer this question. The integrated value of DD for **ML5-3-H$_2$O** is approximately twice the value for **ML5-3-Cl**, while the volume of the basins remains rather similar. As a consequence, the mean value of the DD is higher for **ML5-3-H$_2$O**: the associated vacancy exhibits a higher electrophilicity than the one on **ML5-3-Cl**. The water molecule should then be more stabilised in **3-H$_2$O** than in **3-Cl**, and as such to be less easily replaced: we retrieve a KTE.

This is also confirmed at the NOCV level, as sketched on figure 6. In both cases, a basin of electron density relocation is observed between the incoming water and the rhodium cation, indicating the formation of a σ bond. Further reorganisation of electron density is observed on the remaining of the ligand. It can be
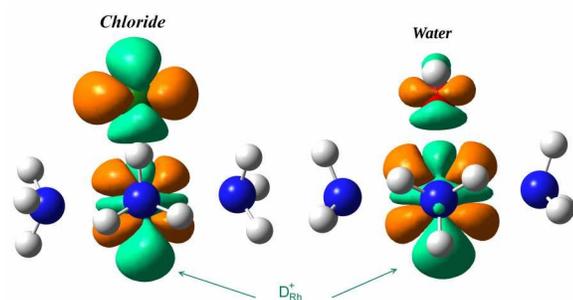
Fig. 5 DD isosurfaces for the [ML$_5$] fragments built from **3-Cl** (left) and **3-H$_2$O** (right). Same colour scheme and isovalues as in figure 3. Cl atoms are represented in olive, and green arrows point towards the D^+_{Rh} domains.

assigned here also to a withdrawal of excess electron density that was transferred from the ligands to the metal cation, in order to counteract the coordination vacancy. Coordination of water to **ML5-3-H$_2$O** is associated to a transfer of 0.48 electrons, and an energetic stabilisation of 31.0 kcal/mol.

On the other hand, coordination to **ML5-3-Cl** leads only to the transfer of 0.36 electrons and a stabilisation of 16.7 kcal/mol. The incoming water molecule is then much less stabilised in **3-Cl** and one expects its replacement to proceed much quickly: the KTE is retrieved.
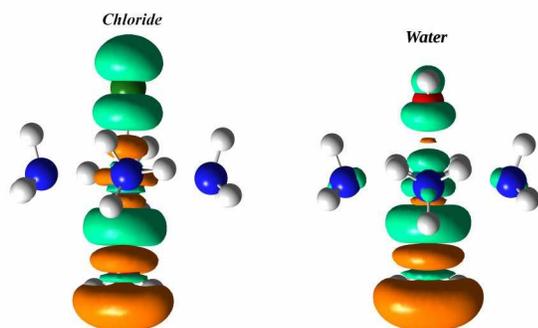
Fig. 6 Deformation density associated to the first NOCV pair for the coordination of H$_2$O to **ML5-3-Cl** (left) and **ML5-3-H$_2$O** (right). Same colour scheme and isovalues as figure 4, the incoming ligands being located on the lower side (same orientation as in figure 5).

3.3.2 Another KTE complex: [Co(en)$_2$(H$_2$O)X]$^{n+}$

Let us now consider the case of [Co(en)$_2$(H$_2$O)X]$^{n+}$, with X = OH$^-$, n=2 (**4-OH**) and X = SO$_3^{2-}$, n=1 (**4-SO$_3$**) (en=ethylenediamine). This complex involves a π-acceptor ligand, and thus differences in the aspect of the DD with respect to the previous cases might be expected. It was shown experimentally that water substitution is 2000 times faster in **4-SO$_3$** than in **4-OH**[65,66]. In the same spirit as previously, we built two [ML$_5$] fragments by removing the coordinated water molecule of **4-SO$_3$** (**ML5-4-SO$_3$**) and **4-OH** (**ML5-4-OH**), and computed the DD.

The results are presented on figure 7. The metal cation here also bears a nucleophilic domain with a shape reminiscent of a d-type metal AO, and an electrophilic domain developing towards the vacancy. In the case of **4-SO$_3$** the domains look quite dis-

torted, and the electrophilic one is very small as compared to **4-OH**. This apparent lower electrophilicity is retrieved in numerical values from the condensation, recapped in table 4.

The integrated value is indeed between 3 to 4 times larger for **ML5-4-OH** than **ML5-4-SO$_3$**, and the mean value is also much larger. More electrophilicity is then seen on the vacancy when the *trans* ligand is hydroxo, thus suggesting the coordinated water would be much more stabilised in **4-OH** than in **4-SO$_3$**.
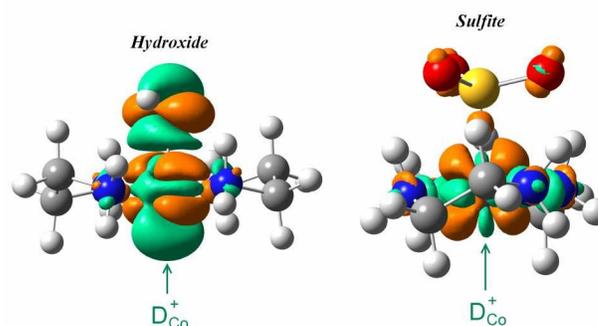
Fig. 7 DD isosurfaces for the [ML$_5$] fragments built from **4-OH** (left) and **4-SO$_3$** (right). Same colours scheme and isovalues as in figure 3. Green arrows point towards the D^+_{Co} domains, hydroxide and sulfite being highlighted.

This is also completely retrieved at the NOCV level, as represented on figure 8. During coordination of water to the [ML$_5$] fragments, a basin of electron density relocation is observed between H$_2$O and the cobalt atom, indicating as previously the formation of a σ bond. From the graphical point of view, this relocation of electron density is much larger for **4-OH** than in **4-SO$_3$**.

Table 4 DD condensation for [ML$_5$] fragments deriving from complex **4**. All values in atomic units.

	4-OH	4-SO$_3$
$\Delta s(D^+_{Co})$	73.7	20.0
$V(D^+_{Co})$	33.6	13.4
$\overline{\Delta s(D^+_{Co})}$	2.19	1.49

This is retrieved in the numerical values: coordination of water to **4-OH** involves the relocation of 0.33 electrons and a stabilisation of 15.6 kcal/mol. On the other hand, only 0.22 electrons are transferred during coordination to **4-SO$_3$**, with a stabilisation of 6.3 kcal/mol. As a result, coordination of water is much weaker when *trans* to a sulfito ligand, as compared to hydroxo. One would then expect an easier substitution in that case, as observed experimentally.

4 A quantitative scale

From the previous examples, it appears that our methodology permits to highlight the *trans* effects by either differentiating the *cis* and *trans* positions in a given complex, or by comparing two different *trans* orienting ligands. Furthermore, using our recently devised topological partition of the DD we have been able to relate these effects to differences in electrophilicity on given sites

Hydroxide   *Sulfite*
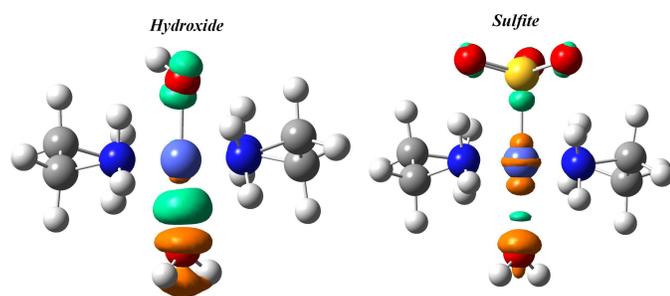
Fig. 8 Deformation density associated to the first NOCV pair for the coordination of H_2O to **ML5-4-OH** (left) and **ML5-4-SO$_3$** (right). Same colours scheme, orientations and isovalues as figure 2. The incoming water molecule is located on the lower side.

around the metal cation: systematically, lower values were observed on the position where either a STE or a KTE is expected. This is in perfect line with the conclusions of both Chval and De Proft (and co-workers)[31,32]. The former interpreted the *trans* effects as a "competition between the ligands [...] for the opportunity to donate their electron density to the central" metal cation. On the other hand, the latter proposed that a very efficient donation from the *trans* orienting ligand would translate in an electron density accumulation on the *trans* position, which in turn would induce a strong Pauli repulsion with the *trans* ligand, hence destabilising it. It is obvious that both effects would translate in a smaller electrophilicity on the *trans* position with respect to the strongest donor, as observed.

We intend to show in this last part that this electrophilicity can be used to draw a quantitative scale of the *trans* orienting ligands. This scale resembles the experimental one, which is roughly the following (ranking from high STE to low)[2,3,6]:

$$CH_3^- \approx CO \approx NO_2^- > Cl^- > Pyridine > NH_3 > H_2O$$

Let us then consider complex **3** derivatives $[Rh(NH_3)_4(H_2O)X]^{n+}$ with X belonging to the previous series. If we apply the same methodology as in part 3.3, for every fragment $[Rh(NH_3)_4X]^{n+}$ an electrophilic domain is observed on the metal cation, pointing towards the vacancy. Because the shapes of the DD are always the same, in the following we will only discuss the condensed values. They are all summed up in table 5.

As previously, the ranges of both the integrated DD values and the volume of the electrophilic domains are large. On the other hand, the mean values are rather close to unity (ranging from 0.36 to 1.74 a.u.), with a smaller dispersion. Furthermore, as we discussed in the "Theoretical backgrounds" part, these mean values are also more readily understandable than mere integrated values, having the same units than the DD. In our context, they are the best index to build a quantitative scale.

Ranking the ligands from the lowest to the highest mean values $\overline{\Delta s(D_{Rh}^+)}$, one obtains:

$$NO_2^- < CH_3^- \approx CO < NH_3 < Cl^- < Pyridine < H_2O$$

which is close to the experimental series. Noticeably, one re-

Table 5 DD condensation for [ML$_5$] fragments deriving from complex **3**. All values in atomic units.

X =	$\Delta s(D_{Rh}^+)$	$V(D_{Rh}^+)$	$\overline{\Delta s(D_{Rh}^+)}$
CH_3^-	9.5	10.7	0.88
CO	14.1	15.8	0.89
NO_2^-	1.6	4.5	0.36
Pyridine	36.4	24.9	1.47
NH_3	18.5	17.9	1.03
Cl^-	21.9	19.2	1.14
H_2O	43.9	25.2	1.74

trieves that the high field ligands are associated to the lowest electrophilicity, and as such to stronger *trans* effects. The order of the weak *trans* orienting ligands seems on the other hand less correctly reproduced.

This was rather expected, since the experimental series is averaged over large sets of complexes, studied in rather different conditions (temperature, solvents). This experimental series provides a rough trend, rather than a precise order, and many exceptions are known[6]. As such, our computed ranking might actually bear much meaning than the experimental series. Noticeably, it should be possible to isolate the contribution of each experimental parameter - temperature, pressure, solvent - to the overall *trans* effect, using a purely computational framework. Such a study goes beyond the scope of this paper, and may be the subject of a following survey.

In order to confirm our calculated scale, at least on the strong-field part of the series, we decided to study another series of complexes[67], $[Ru(NH_3)_5X]^{n+}$ (5) with the same X - to the exception of NH_3, which would be meaningless, since no differentiation would be seen due to the octahedral symmetry. The shape of the DD is also very similar to the previous examples, and we will only discuss the numerical values, summarised in table 6. The order of the ligands, ranked from the lowest to the highest $\overline{\Delta s(D_{Ru}^+)}$ is:

$$NO_2^- < CH_3^- < CO < Pyridine < Cl^- < H_2O$$

As one can remark, the same order as previously is obtained for the lowest contributions, NO_2^-, CH_3^- and CO being in both cases strong *trans* orienting ligands. On the other hand, the order of the weak *trans* orienting ligands is different, being closer to the experimental trends.

Table 6 DD condensation for [ML$_5$] fragments deriving from complex **5**. All values in atomic units.

X =	$\Delta s(D_{Ru}^+)$	$V(D_{Ru}^+)$	$\overline{\Delta s(D_{Ru}^+)}$
CH_3^-	22.4	28.9	0.77
CO	18.3	21.5	0.85
NO_2^-	21.0	35.2	0.60
Pyridine	29.4	26.1	1.13
Cl^-	36.3	26.4	1.37
H_2O	43.2	30.6	1.41

5　Conclusions

In conclusion, we showed that it is possible to retrieve the *trans* effects for some octahedral complexes, using tools from conceptual DFT or close paradigms. It seems that both effects are due to differences in the way electron density is likely to reorganise in the complex, under the influence of a specific ligand. This ligand, by decreasing the need for electron density on the *trans* position, weakens the associated metal-ligand bond and as such leads to an increase in the bond length or kinetics. Monitoring the electrophilicity allows then to characterise and quantify the *trans* effects, and permitted us to build a quantitative scale of the *trans* orienting ligands following a systematic approach. This scale, although not perfect, follows rather closely the experimental trends. This suggests that *trans* effects are primarily controlled by the electron density donation properties of the ligands on the *trans* position. The rather large diversity of studied cases, either in transition metal series and ligand types, suggests these findings are quite general.

Both *trans* effects are often encountered in coordination chemistry, but failed to be precisely understood. We hope our results will help to change this fact, and may for instance allow to rationally design molecular devices for specific drug delivery or catalysis, basing on KTE. On a wider scope, we hope our combined DD/NOCV study will stimulate a further research effort, in order to enlighten the physics beneath metal-ligands interaction in coordination complexes.

References

1　I. I. Chernayev, *Ann. Inst. Platine*, 1926, **4**, 243–275.

2　J. E. Huheey, E. A. Keiter and R. L. Keiter, *Inorganic Chemistry (French Edition)*, DeBoeck Université, 1993.

3　D. F. Shriver, P. W. Atkins and C. H. Langford, *Inorganic Chemistry (2nd Edition)*, Oxford University Press, 1994.

4　J. K. Burdett and T. A. Albright, *Inorg. Chem.*, 1979, **18**, 2112–2120.

5　J. V. Quagliano and L. Schubert, *Chem. Rev.*, 1952, **50**, 201–266.

6　B. J. Coe and S. J. Glenwright, *Coord. Chem. Rev.*, 2000, **203**, 5–80.

7　K. Krogh-Jespersen, M. D. Romanelli, J. H. Melman, T. J. Emge and J. G. Brennan, *Inorg. Chem.*, 2010, **49**, 552–560.

8　H. Chermette, K. Rachedi and F. Volatron, *J. Mol. Struct. THEOCHEM*, 2006, **762**, 109–121.

9　A. J. Lewis, K. C. Mullane, E. Nakamaru-Ogiso, P. J. Carroll and J. E. Schelter, *Inorg. Chem.*, 2014, **53**, 6944–6953.

10　V. Tognetti, A. Boulangé, P. A. Peixoto, X. Franck and L. Joubert, *J. Mol. Model.*, 2014, **20**, 2342.

11　P. K. Sajith and C. H. Suresh, *Inorg. Chem.*, 2012, **51**, 967–977.

12　Y.-X. Jia, B.-B. Li, Y. Li, S. A. Pullarkat, H. Hirao and P.-H. Leung, *Organometallics*, 2014, **53**, 6053–6058.

13　G. Zhang, K. Chen, H. Chen, J. Yao and S. Shaik, *Inorg. Chem.*, 2013, **52**, 5088–5096.

14　J. Kwak, Y. Ohk, Y. Jung and S. Chang, *J. Am. Chem. Soc.*, 2012, **134**, 17778–17788.

15　A. P. Hunt and N. Lehnert, *Acc. Chem. Res.*, 2015, **48**, 2117–2125.

16　D. Lieb, F. C. Friedel, M. Yawer, A. Zahl, M. M. Khusniyarov, F. W. Heinemann and I. Ivanovic-Burmazovic, *Inorg. Chem.*, 2012, **52**, 222–236.

17　N. Dolker, F. Maseras and A. Lledos, *J. Phys. Chem. B*, 2003, **107**, 306–315.

18　K. Czarnecki, S. Nimri, Z. Gross, L. M. Proniewicz and J. R. Kincald, *J. Am. Chem. Soc.*, 1996, **118**, 2929–2935.

19　Y. Zhang, Z. Guo and X.-Z. You, *J. Am. Chem. Soc.*, 2001, **123**, 9378–9387.

20　M.-H. Baik, R. A. Friesner and S. J. Lippard, *J. Am. Chem. Soc.*, 2003, **125**, 14082–14092.

21　J. Raber, C. Zhu and L. A. Eriksson, *J. Phys. Chem. B*, 2005, **109**, 11006–11015.

22　I. I. Chernayev, *Ann. Inst. Platine.*, 1927, **5**, 109.

23　A. A. Grinberg, *Ann. Inst. Platine.*, 1932, **10**, 58.

24　A. A. Grinberg, *Acta. Phys. Chim.*, 1935, **3**, 573.

25　H. S. La Pierre, M. Rosenzweig, B. Kosog, C. Hauser, F. W. Heinemann, S. T. Liddle and K. Meyer, *Chem. Commun.*, 2015, doi:10.1039/C5CC07211.

26　J. Chatt and L. A. Duncanson, *J. Chem. Soc.*, 1953, 2939–2947.

27　M. J. S. Dewar, *Bull. Soc. Chim. Fr.*, 1951, **18**, C71.

28　B. A. Bovykin, *Teor. i Eksp. Khimica*, 1974, **10**, 238–240.

29　A. Pidcock, R. E. Richards and L. M. Venanzi, *J. Chem. Soc. A*, 1968, 1970–1973.

30　M. P. Mitoraj, H. Zhu, A. Michalak and T. Ziegler, *Int. J. Quantum Chem.*, 2009, **109**, 3379–3386.

31　Z. Chval, M. Sip and J. V. Burda, *J. Comput. Chem.*, 2008, **29**, 2370–2381.

32　B. Pinter, V. Van Speybroeck, M. Waroquier, P. Geerlings and F. De Proft, *Phys. Chem. Chem. Phys.*, 2013, **15**, 17354–17365.

33　P. Geerlings, F. De Proft and W. Langenaeker, *Chem. Rev.*, 2003, **103**, 1793–1873.

34　H. Chermette, *J. Comput. Chem.*, 1998, **20**, 129–154.

35　J. L. Gazquez, *J. Mex. Chem. Soc.*, 2008, **52**, 3–10.

36　R. G. Parr and W. Yang, *J. Am. Chem. Soc.*, 1984, **106**, 4049–4050.

37　C. Morell, A. Grand and A. Toro-Labbé, *J. Phys. Chem. A*, 2005, **109**, 205–212.

38　P. Geerlings and F. De Proft, *Phys. Chem. Chem. Phys.*, 2008, **10**, 3028–3042.

39　J. I. Martinez-Arraya, *J. Math. Chem.*, 2015, **53**, 451–465.

40　M. Mitoraj and A. Michalak, *J. Mol. Model.*, 2007, **13**, 347–355.

41　A. Michalak, M. Mitoraj and T. Ziegler, *J. Phys. Chem. A*, 2008, **112**, 1933–1939.

42　M. P. Mitoraj, M. Parafiniuk, M. Srebro, M. Handzlik, A. Buczek and A. Michalak, *J. Mol. Model.*, 2011, **17**, 2337–2352.

43　F. De Proft, V. Forquet, B. Ourri, H. Chermette, P. Geerlings

and C. Morell, *Phys. Chem. Chem. Phys.*, 2015, **17**, 9359–9368.

44 B. Pinter, N. Nagels, W. A. Herrebout and F. De Proft, *Chem. Eur. J.*, 2013, **19**, 519–530.

45 C. Morell, A. Grand and A. Toro-Labbé, *Chem. Phys. Lett.*, 2006, **425**, 342–346.

46 P. Geerlings, P. W. Ayers, A. Toro-Labbé, P. K. Chattaraj and F. De Proft, *Acc. Chem. Res.*, 2012, **53**, 683–695.

47 J. M. del Campo and J. I. Martinez-Arraya, *Propellants Explos. Pyrotech.*, 2014, **39**, 890–896.

48 J. I. Martinez-Arraya, *J. Mol. Model.*, 2013, **19**, 2715–2722.

49 V. Tognetti, C. Morell, P. W. Ayers, L. Joubert and H. Chermette, *Phys. Chem. Chem. Phys.*, 2013, **15**, 14465–14475.

50 F. Guégan, P. Mignon, V. Tognetti, L. Joubert and C. Morell, *Phys. Chem. Chem. Phys.*, 2014, **16**, 15558–15569.

51 L.-J. Jouanno, V. Di Mascio, V. Tognetti, L. Joubert, C. Sabot and P.-Y. Renard, *J. Org. Chem.*, 2014, **19**, 1303–1319.

52 E. Falkowska, V. Tognetti, L. Joubert, P. Jubault, J.-P. Bouillon and X. Pannecoucke, *RSC Adv.*, 2015, **5**, 6864–6868.

53 V. Tognetti, C. Morell and L. Joubert, *J. Comput. Chem.*, 2015, **36**, 648–659.

54 M. Mitoraj and A. Michalak, *Organometallics*, 2007, **26**, 6576–6580.

55 M. P. Mitoraj, A. Michalak and T. Ziegler, *J. Chem. Theory Comput.*, 2009, **5**, 962–975.

56 M. J. Frisch, G. W. Trucks, H. B. Schlegel, G. E. Scuseria, M. A. Robb, J. R. Cheeseman, G. Scalmani, V. Barone, B. Mennucci, G. A. Petersson, H. Nakatsuji, M. Caricato, X. Li, H. P. Hratchian, A. F. Izmaylov, J. Bloino, G. Zheng, J. L. Sonnenberg, M. Hada, M. Ehara, K. Toyota, R. Fukuda, J. Hasegawa, M. Ishida, T. Nakajima, Y. Honda, O. Kitao, H. Nakai, T. Vreven, J. A. Montgomery, Jr., J. E. Peralta, F. Ogliaro, M. Bearpark, J. J. Heyd, E. Brothers, K. N. Kudin, V. N. Staroverov, R. Kobayashi, J. Normand, K. Raghavachari, A. Rendell, J. C. Burant, S. S. Iyengar, J. Tomasi, M. Cossi, N. Rega, J. M. Millam, M. Klene, J. E. Knox, J. B. Cross, V. Bakken, C. Adamo, J. Jaramillo, R. Gomperts, R. E. Stratmann, O. Yazyev, A. J. Austin, R. Cammi, C. Pomelli, J. W. Ochterski, R. L. Martin, K. Morokuma, V. G. Zakrzewski, G. A. Voth, P. Salvador, J. J. Dannenberg, S. Dapprich, A. D. Daniels, Ã. Farkas, J. B. Foresman, J. V. Ortiz, J. Cioslowski and D. J. Fox, *Gaussian 09 Revision D.01*, Gaussian Inc. Wallingford CT 2009.

57 U. Wedig, M. Dolg, H. Stoll and H. Preuss, *Quantum chemistry: the challenge of transition metals and coordination chemistry*, Reidel, Dordrecht, 1986.

58 A. J. H. Wachters, *J. Chem. Phys.*, 1970, **52**, 1033–1036.

59 C. W. Bauschlicher, S. R. Langhoff and L. A. Partridge, H. Barnes, *J. Chem. Phys.*, 1989, **91**, 2399–2411.

60 E. J. Baerends *et al.*, *ADF 2013*, SCM, Theoretical Chemistry, Vrije Universiteit, Amsterdam, The Netherlands.

61 R. Dennington, T. Keith and J. Millam, *GaussView version 5*, Semichem Inc., Shawnee Mission, KS.

62 P. Kofod, P. Harris and S. Larsen, *Inorg. Chem.*, 1997, **5**, 2258–2266.

63 B. Kamenar and C. K. Prout, *J. Chem. Soc.*, 1970, **9**, 2379–2384.

64 L. Monsted and O. Monsted, *Acta Chem. Scand.*, 1984, **A38**, 67–71.

65 D. R. Stranks and J. K. Yandell, *Inorg. Chem.*, 1970, **9**, 751–757.

66 E. N. Maslen and J. K. Yandell, *J. Chem. Soc. Dalt. Trans.*, 1975, 327–329.

67 F. Bottomley, *J. Chem. Soc. Dalt. Trans.*, 1972, 2148–2152.